Supplementary Information

for

Quantum chemical and kinetic study of the reaction between CCl_2 and NO_2 radicals

Nicolás D. Gómez*, María P. Badenes, María E. Tucceri, Carlos J. Cobos

Instituto de Investigaciones Fisicoquímicas Teóricas y Aplicadas (INIFTA).

Departamento de Química. Facultad de Ciencias Exactas. Universidad Nacional de La Plata. CCT La Plata-CONICET. Casilla de Correo 16. Sucursal 4. (1900) La Plata. Argentina. nicodgomez@inifta.unlp.edu.ar

Description of the G4//DFT chemistry model

The steps used in the implementation of the G4//DFT/6-311+G(3df) model chemistry are as follows [1].

(1) The equilibrium structure is obtained at the DFT/6-311+G(3*df*) level.

(2) The DFT/6-311+G(3*df*) equilibrium structure is used to calculate harmonic frequencies.

(3) The DFT/6-311+G(3df) equilibrium structure is used in a series of single point calculations.

(a) Hartree-Fock energy limit:

$$E_{HF/aug-cc-pVnZ} = E_{HF/limit} + B\exp(-\alpha n)$$

(b) Correction for diffuse functions,

$$\Delta E(+) = E[MP4/6-31+G(d)] - E[MP4/6-31G(d)]$$

(c) Correction for higher polarization functions,

$$\Delta E(2df,p) = E[MP4/6-31G(2df,p)] - E[MP4/6-31G(d)]$$

(d) Correction for correlation effects,

$$\Delta E(CC) = E[CCSD(T)-31G(d)] - E[MP4/6-31G(d)]$$

(e) $\Delta E(G3LargeXP) = E[MP2/G3LargeXP] - E[MP2/6-31G(2df,p)] - E[MP2/6-31+G(d)] + E[MP2/6-31G(d)]$

And the combined energy is given by,

$$E_0(G4) = E_e(G4) + E(DFT/6-311+G(3df)\ ZPE)$$

Where

$$E_e(G4) = E[MP4/6-31G(d)] + \Delta E(+) + \Delta E(2df,p) + \Delta E(CC) + \Delta E(G3LargeXP) + \Delta E(HF) + \Delta E(SO) + E(HLC)$$

ΔE(SO) is the spin-orbit correction factor for atomic species, E(*HLC*) is a high level correction factor and ΔE(HF) = E(HF/limit)-E(HF/G3LargeXP).

Table S1. Molecular parameters (bond lengths in Å and bond angles in degrees), harmonic vibrational frequencies (in cm^{-1}) and rotational constants (in cm^{-1}) for species of Figure 1, computed at the M11-L/6-311+G(*3df*) level of theory. Energy (in hartree) calculated with the G4//M11-L/6-311+G(3*df*) chemistry model and spin degeneracies.

Parameter	Value	
r(CCl_1)	1.705	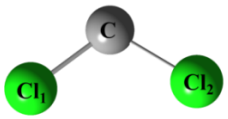
r(CCl_2)	1.705	
∠(Cl_1CCl_2)	109.3	

Rotational constants: 1.690, 0.125, 0.116

Vibrational frequencies: 336, 736, 755

Energy (Electronic+ZPE): -958.140519 (Singlet)

Parameter	Value	**Parameter**	Value
r(CCl_1)	1.644	r(NC)	1.415
r(CCl_2)	1.644	r(NO_1)	1.199
∠(Cl_1CCl_2)	122.1	r(NO_2)	1.199
		∠($NCCl_1$)	119.0
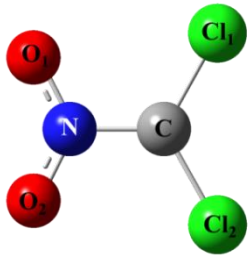		∠(O_1NC)	116.5
		∠(O_2NC)	116.5
		DIH($NCCl_1Cl_2$)	180.0
		DIH(O_1NCCl_1)	0.05
		DIH(O_2NCCl_1)	180.0

Rotational constants: 0.093, 0.089, 0.046

Vibrational frequencies: 95, 233, 247, 290, 475, 502, 709, 813, 1105, 1115, 1378, 1682

Energy (Electronic+ZPE): -1163.220000 (Doublet)

Parameter	Value	**Parameter**	Value
r(CCl_1)	1.659	r(NC)	1.355
r(CCl_2)	1.669	r(NO_1)	1.332
∠(Cl_1CCl_2)	118.1	r(NO_2)	1.205
		∠($NCCl_1$)	121.2
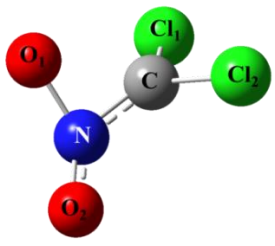		∠(O_1NC)	85.9
		∠(O_2NC)	130.3
		DIH($NCCl_1Cl_2$)	-168.8
		DIH(O_1NCCl_1)	-83.1
		DIH(O_2NCCl_1)	139.3

Rotational constants: 0.098 0.079 0.051

Vibrational frequencies: 936i, 145, 216, 288, 348, 467, 496, 663, 957, 1101, 1200,1603

Energy (Electronic+ZPE): -1163.159148 (Doublet)

Table S1 (cont.). Molecular parameters (bond lengths in Å and bond angles in degrees), harmonic vibrational frequencies (in cm^{-1}) and rotational constants (in cm^{-1}) for species of Figure 1, computed at the M11-L/6-311+G(*3df*). Energy (in hartree) calculated with the G4//M11-L/6-311+G(3*df*) chemistry model.

Parameter	Value	**Parameter**	Value
r(CCl_1)	1.696	r(CO_1)	2.346
r(CCl_2)	1.699	r(NO_1)	1.178
∠(Cl_1CCl_2)	110.8	r(NO_2)	1.167
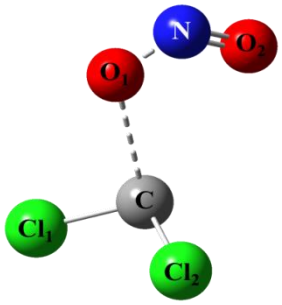		∠(Cl_1CO_1)	101.0
		∠(CO_1N)	103.9
		∠(O_1NO_2)	130.2
		DIH($Cl_2Cl_1CO_1$)	-106.4
		DIH(Cl_1CO_1N)	-146.2
		DIH(CO_1NO_2)	-0.5
Rotational constants: 0.103, 0.050, 0.038			
Vibrational frequencies: 89i, 19, 83, 112, 176, 242, 339, 669, 762, 793, 1405, 1772			
Energy (Electronic+ZPE): -1163.155428 (Doublet)			
Parameter	Value	**Parameter**	Value
r(CCl_1)	1.687	r(CO_1)	1.997
r(CCl_2)	1.693	r(NO_1)	1.209
∠(Cl_1CCl_2)	113.8	r(NO_2)	1.173
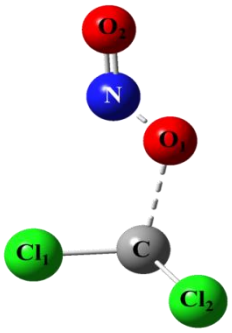		∠(Cl_1CO_1)	98.9
		∠(CO_1N)	109.2
		∠(O_1NO_2)	124.7
		DIH($Cl_2Cl_1CO_1$)	108.5
		DIH(Cl_1CO_1N)	-154.7
		DIH(CO_1NO_2)	175.6
Rotational constants: 0.121, 0.049, 0.036			
Vibrational frequencies: 578i, 75, 105, 187, 232, 294, 338, 603, 811, 867, 1186, 1680			
Energy (Electronic+ZPE): -1163.131190 (Doublet)			

Table S1 (cont.). Molecular parameters (bond lengths in Å and bond angles in degrees), harmonic vibrational frequencies (in cm^{-1}) and rotational constants (in cm^{-1}) for species of Figure 1, computed at the M11-L/6-311+G(*3df*). Energy (in hartree) calculated with the G4//M11-L/6-311+G(3*df*) chemistry model.

Parameter	Value	**Parameter**	Value
r(CCl_1)	1.689	r(CO_1)	1.334
r(CCl_2)	1.687	r(CO_2)	1.797
∠(Cl_1CCl_2)	114.5	r(NO_2)	1.245
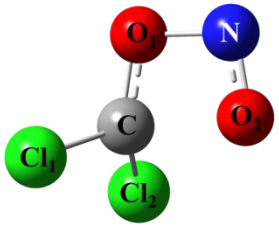		∠(Cl_1CO_1)	113.8
		∠(O_1CO_2)	79.1
		∠(CO_2N)	83.6
		DIH($C_2Cl_1CO_1$)	142.0
		DIH($Cl_1O_1CO_2$)	-125.9
		DIH(O_1CO_2N)	4.0
Rotational constants: 0.102, 0.084, 0.055			
Vibrational frequencies: 1292i, 141.6, 227, 297, 316, 442, 526, 665, 891, 1004, 1110, 1233			
Energy (Electronic+ZPE): -1163.178187 (Doublet)			
Parameter	Value	**Parameter**	Value
r(CCl_1)	1.919	r(NC)	1.734
r(CCl_2)	1.734	r(O_1C)	1.369
∠(Cl_1CCl_2)	124.7	r(O_2C)	1.369
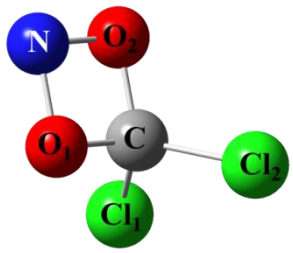		∠($NCCl_1$)	110.5
		∠(NCO_1)	45.8
		∠(NCO_2)	45.8
		DIH(NCl_1CCl_2)	180.0
		DIH(Cl_2NCO_1)	90.0
		DIH(Cl_2NCO_2)	-90.0
Rotational constants: 0.098, 0.094, 0.058			
Vibrational frequencies: 181, 277, 289, 421, 441, 496, 900, 947, 1020, 1097, 1126, 1196			
Energy (Electronic+ZPE): -1163.219735 (Doublet)			

Table S1 (cont.). Molecular parameters (bond lengths in Å and bond angles in degrees), harmonic vibrational frequencies (in cm^{-1}) and rotational constants (in cm^{-1}) for species of Figure 1, computed at the M11-L/6-311+G(*3df*). Energy (in hartree) calculated with the G4//M11-L/6-311+G(3*df*) chemistry model.

Parameter	Value	**Parameter**	Value
r(CCl_1)	1.636	r(CN)	1.292
r(CCl_2)	2.173	r(NO_1)	1.196
∠(Cl_1CCl_2)	139.7	r(NO_2)	1.370
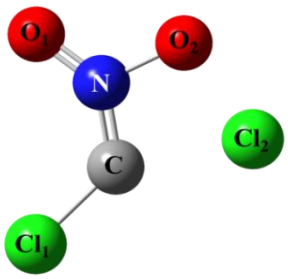		∠(Cl_1CN)	124.8
		∠(CNO_1)	134.2
		∠(CNO_2)	108.5
		DIH(Cl_2Cl_1CN)	-129.9
		DIH(Cl_1CNO_1)	-28.0
		DIH(O_1CNO_2)	-172.5
Rotational constants: 0.122, 0.064, 0.042			
Vibrational frequencies: 735i, 108, 173, 211, 346, 495, 575, 591, 808, 990, 1333, 1714			
Energy (Electronic+ZPE): -1163.087271 (Doublet)			

Parameter	Value
r(CCl)	1.611
r(CN)	1.157
r(NO)	1.172
∠(ClCN)	151.1
∠(CNO)	169.3
DIH(ClCNO)	180.0

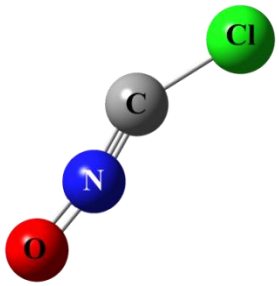

Rotational constants: 11.681, 0.090, 0.090
Vibrational frequencies: 163, 436, 481, 686, 1472, 2420
Energy (Electronic+ZPE): -627.980445 (Singlet)

Table S1 (cont.). Molecular parameters (bond lengths in Å and bond angles in degrees), harmonic vibrational frequencies (in cm^{-1}) and rotational constants (in cm^{-1}) for species of Figure 1, computed at the M11-L/6-311+G(*3df*). Energy (in hartree) calculated with the G4//M11-L/6-311+G(3*df*) chemistry model.

	Parameter	Value
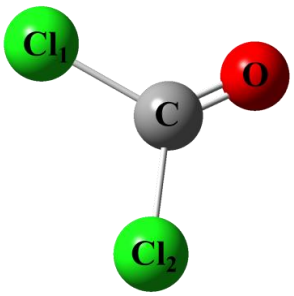	r(CO)	1.156
	r(CCl_1)	1.718
	r(CCl_2)	1.717
	∠($OCCl_1$)	124.2
	∠($OCCl_2$)	124.2
	DIH(Cl_1OCCl_2)	180.0
Rotational constants: 0.272, 0.119, 0.083		
Vibrational frequencies: 313, 459,600, 613, 869, 1956		
Energy (Electronic+ZPE): -1033.447900 (Singlet)		
Parameter	Value	
r(NO_1)	1.167	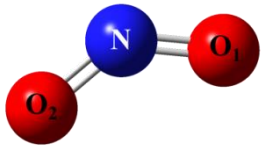
r(NO_2)	1.167	
∠(O_1CO_2)	134.2	
Rotational constants: 1.690, 0.125, 0.116		
Vibrational frequencies: 805, 1474, 1835		
Energy (Electronic+ZPE): -205.016698 (Doublet)		
Parameter	Value	
r(ClO)	1.533	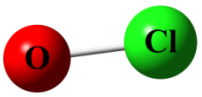
Rotational constants: 0.653		
Vibrational frequencies: 913		
Energy (Electronic+ZPE): -535.158436 (Doublet)		
Parameter	Value	
r(NO)	1.127	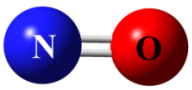
Rotational constants: 1.778		
Vibrational frequencies: 2067		
Energy (Electronic+ZPE): -129.857439 (Doublet)		

Table S2. Enthalpies of formation (kcal mol^{-1}) of CCl_2NO_2 calculated by isodesmic reactions with the different functionals employed. b: 6-311+G(3*df*).

Isodesmic reaction	ΔH_f(0 K)				
	B3LYP/b	M08-HX/b	MN15/b	MN15-L/b	PW6B95/b
$CCl_2+C_2H_5NO_2 \rightarrow CCl_2NO_2+C_2H_5$	18.0	20.5	19.5	22.0	19.3
$CHCl_2+C_2H_5NO_2 \rightarrow CCl_2NO_2+C_2H_6$	16.9	17.9	15.8	15.3	16.5
$2CH_2Cl+C_2H_5NO_2 \rightarrow CCl_2NO_2+C_2H_5+CH_4$	23.5	25.4	22.5	20.7	23.0
$2CH_2Cl+C_2H_5NO_2 \rightarrow CCl_2NO_2+C_2H_6+CH_3$	24.1	25.3	23.0	21.0	23.8
$CCl_3+C_2H_5NO_2 \rightarrow CCl_2NO_2+C_2H_5Cl$	21.2	22.3	21.1	19.8	21.4
$CH_2CCl_2+C_2H_5NO_2 \rightarrow CCl_2NO_2+C_3H_7$	17.6	21.5	20.2	18.2	19.6
$CH_3CCl_2+C_2H_5NO_2 \rightarrow CCl_2NO_2+C_3H_8$	21.7	22.7	21.4	20.0	21.4
$CH_2CCl_3+C_2H_5NO_2 \rightarrow CCl_2NO_2+C_3H_7Cl$	20.7	23.2	21.3	20.7	19.7
$CCl_2+CH_3NO_2 \rightarrow CCl_2NO_2+CH_3$	19.9	20.9	20.4	22.4	20.6
$CHCl_2+CH_3NO_2 \rightarrow CCl_2NO_2+CH_4$	18.1	18.5	16.3	15.4	17.1
$2CHCl+CH_3NO_2 \rightarrow CCl_2NO_2+CH_4+CH$	20.6	20.4	22.2	22.8	20.2
$2CHCl+CH_3NO_2 \rightarrow CCl_2NO_2+CH_2+CH_3$	20.6	20.9	21.8	21.5	21.8

Table S2 (cont). Enthalpies of formation (kcal mol^{-1}) of CCl_2NO_2 calculated by isodesmic reactions with the different functionals employed. b: 6-311+G(3*df*).

Isodesmic reaction	ΔH_f(0 K)			
	BMK/b	M06-2X/b	MN12-L/b	MN12-SX/b
$CCl_2+C_2H_5NO_2 \rightarrow CCl_2NO_2+C_2H_5$	22.6	21.3	22.7	22.7
$CHCl_2+C_2H_5NO_2 \rightarrow CCl_2NO_2+C_2H_6$	19.7	18.6	14.1	15.8
$2CH_2Cl+C_2H_5NO_2 \rightarrow CCl_2NO_2+C_2H_5+CH_4$	25.8	26.2	19.0	22.3
$2CH_2Cl+C_2H_5NO_2 \rightarrow CCl_2NO_2+C_2H_6+CH_3$	26.0	26.2	20.3	23.0
$CCl_3+C_2H_5NO_2 \rightarrow CCl_2NO_2+C_2H_5Cl$	22.7	22.5	19.6	21.0
$CH_2CCl_2+C_2H_5NO_2 \rightarrow CCl_2NO_2+C_3H_7$	22.0	22.6	20.2	20.5
$CH_3CCl_2+C_2H_5NO_2 \rightarrow CCl_2NO_2+C_3H_8$	24.2	23.3	20.1	20.9
$CH_2CCl_3+C_2H_5NO_2 \rightarrow CCl_2NO_2+C_3H_7Cl$	23.6	23.5	19.4	21.3
$CCl_2+CH_3NO_2 \rightarrow CCl_2NO_2+CH_3$	23.5	21.3	23.7	23.8
$CHCl_2+CH_3NO_2 \rightarrow CCl_2NO_2+CH_4$	20.5	18.7	13.9	16.2
$2CHCl+CH_3NO_2 \rightarrow CCl_2NO_2+CH_4+CH$	22.0	21.0	24.7	23.6
$2CHCl+CH_3NO_2 \rightarrow CCl_2NO_2+CH_2+CH_3$	23.5	21.3	22.1	22.9

Table S2 (cont). Enthalpies of formation (kcal mol^{-1}) of CCl_2NO_2 calculated by isodesmic reactions with the different functionals employed. b: 6-311+G(3*df*).

Isodesmic reaction	ΔH_f(0 K)			
	M11-L/b	CAM-B3LYP/b	SOGGA11/b	ωB97X-D
$CCl_2+C_2H_5NO_2 \rightarrow CCl_2NO_2+C_2H_5$	21.4	16.6	19.9	19.3
$CHCl_2+C_2H_5NO_2 \rightarrow CCl_2NO_2+C_2H_6$	13.0	17.8	17.5	17.9
$2CH_2Cl+C_2H_5NO_2 \rightarrow CCl_2NO_2+C_2H_5+CH_4$	16.3	25.2	23.3	25.1
$2CH_2Cl+C_2H_5NO_2 \rightarrow CCl_2NO_2+C_2H_6+CH_3$	17.8	25.6	25.3	25.4
$CCl_3+C_2H_5NO_2 \rightarrow CCl_2NO_2+C_2H_5Cl$	19.6	22.4	21.0	22.4
$CH_2CCl_2+C_2H_5NO_2 \rightarrow CCl_2NO_2+C_3H_7$	15.4	17.8	18.6	19.1
$CH_3CCl_2+C_2H_5NO_2 \rightarrow CCl_2NO_2+C_3H_8$	18.3	23.1	22.5	22.6
$CH_2CCl_3+C_2H_5NO_2 \rightarrow CCl_2NO_2+C_3H_7Cl$	17.2	21.5	20.1	21.0
$CCl_2+CH_3NO_2 \rightarrow CCl_2NO_2+CH_3$	23.7	17.8	22.7	20.9
$CHCl_2+CH_3NO_2 \rightarrow CCl_2NO_2+CH_4$	13.6	18.6	18.3	19.1
$2CHCl+CH_3NO_2 \rightarrow CCl_2NO_2+CH_4+CH$	22.2	18.5	22.1	20.8
$2CHCl+CH_3NO_2 \rightarrow CCl_2NO_2+CH_2+CH_3$	21.7	18.8	23.9	21.4

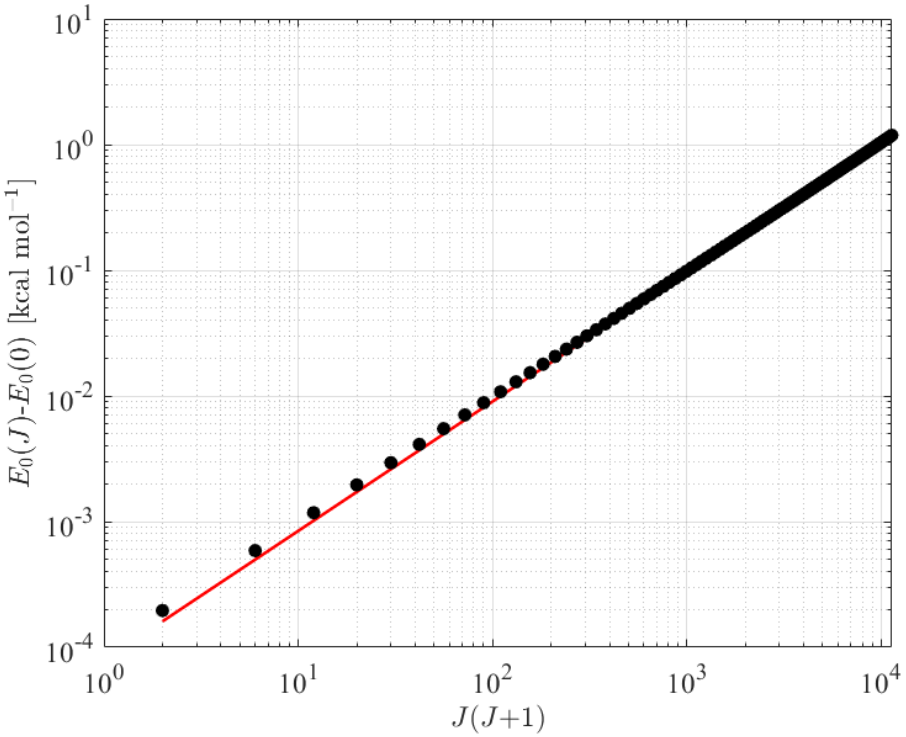

Figure S1. Centrifugal barrier as a function of $J(J+1)$ at the M11-L/6-311+G(3*df*) level. Fit performed with the expression $C_v J(J+1)^v$.

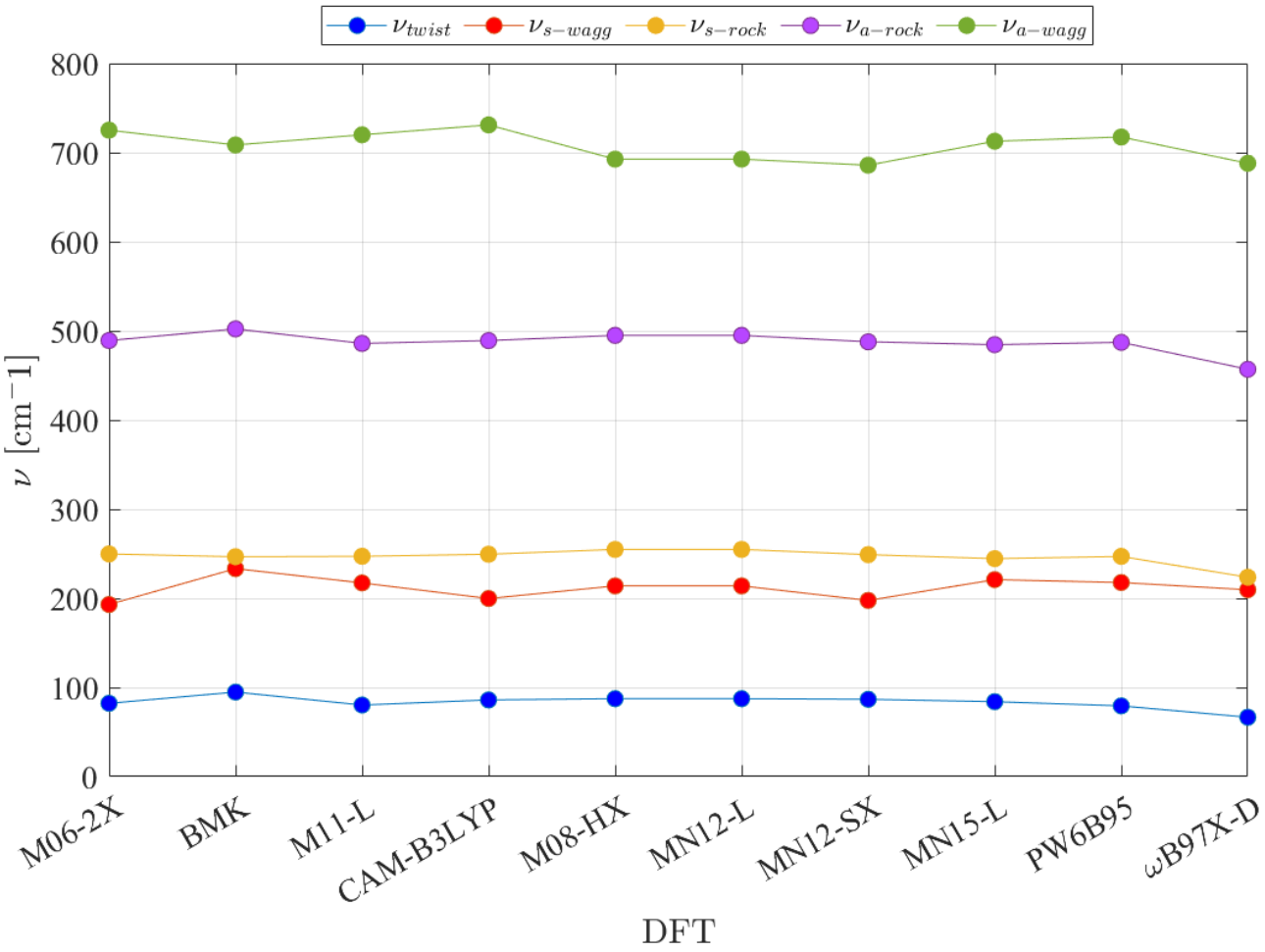

Figure S2. Frequencies of the transitional modes calculated with different DFT models coupled with the 6-311+G(*3df*) basis set.

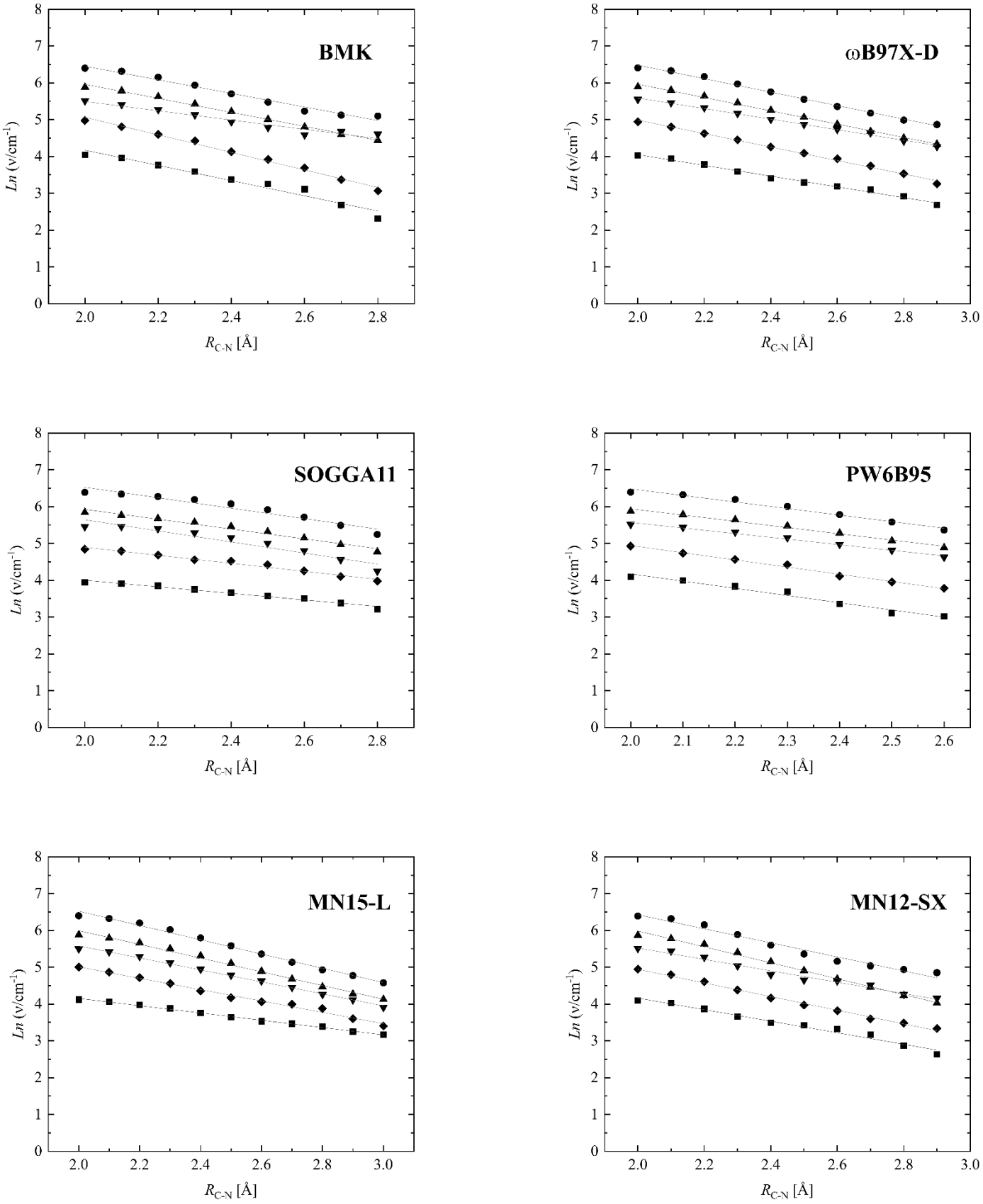

Figure S3. Vibrational frequencies corresponding to the transitional modes as a function of the N-C bond length at the DFT/6-311+G(3*df*) level of theory. ■: Torsion. ♦:Symmetric Rocking. ▼: Symmetric wagging. ▲: Asymmetric Rocking. ●: Asymmetric wagging.

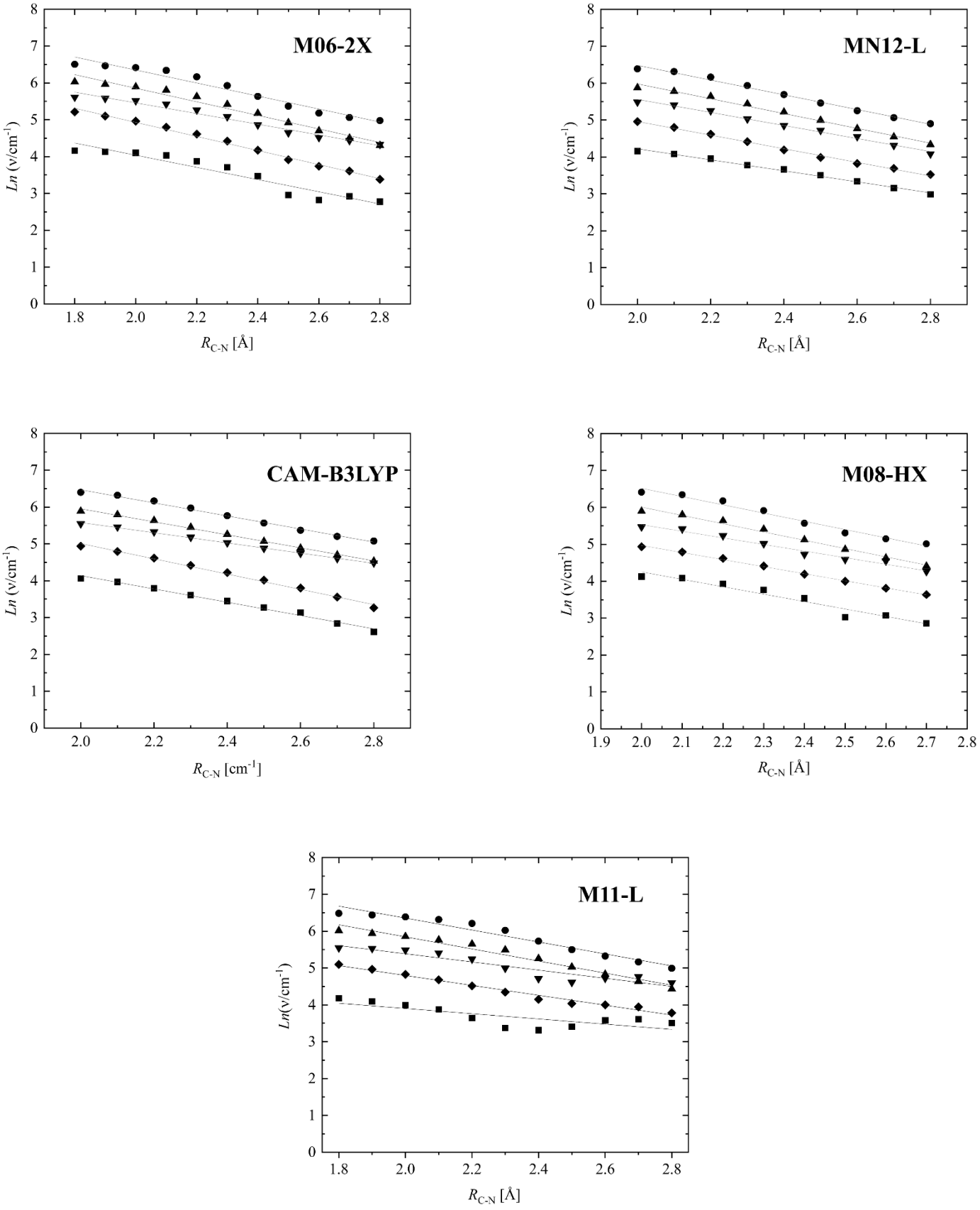

Figure S3 (cont.). Vibrational frequencies corresponding to the transitional modes as a function of the N-C bond length at the DFT/6-311+G(3*df*) level of theory. ■: Torsion. ♦: Symmetric Rocking. ▼: Symmetric wagging. ▲: Asymmetric Rocking. ●: Asymmetric wagging.

Table S3. Looseness parameter, α (in Å^{-1}), of the transitional modes as determined by DFT/6-311+G(*3df*) level of theory. Morse parameter, β (in Å^{-1}), determined by G4//DFT/6-311+G(*3df*) level of theory.

DFT	α_{twist}	$\alpha_{\text{s-rock}}$	$\alpha_{\text{s-wagg}}$	$\alpha_{\text{a-rock}}$	$\alpha_{\text{a-wagg}}$	β
M06-2X	1.65	1.91	1.45	1.84	1.76	4.46
BMK	2.07	2.38	1.26	1.90	1.85	4.44
M11-L	0.71	1.34	1.11	1.64	1.62	4.42
CAM-B3LYP	1.80	2.07	1.38	1.76	1.77	4.24
M08-HX	2.01	1.91	1.79	2.24	2.15	4.40
MN12-L	1.49	1.85	1.77	2.01	2.00	4.36
MN12-SX	1.57	1.85	1.55	2.16	1.91	4.43
MN15-L	1.00	1.54	1.63	1.86	1.94	4.69
PW6B95	1.96	1.95	1.52	1.70	1.78	4.30
ωB97X-D	1.45	1.83	1.44	1.81	1.83	4.36
SOGGA11	0.89	1.09	1.50	1.33	1.42	4.53
Mean ± σ	**1.51 ± 0.47**	**1.79 ± 0.35**	**1.49 ± 0.20**	**1.84 ± 0.24**	**1.82 ± 0.19**	**4.42 ± 0.12**

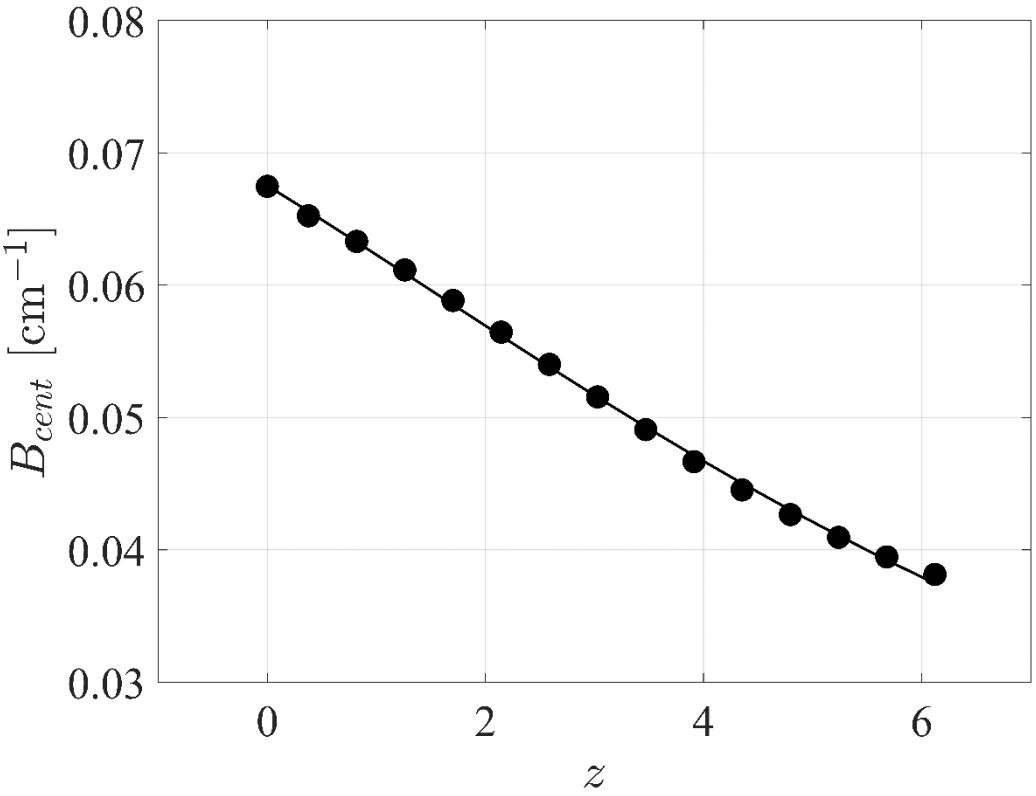

Figure S4. Centrifugal rotational constant as a function of the C-N bond length at the M11-L/6-311+G(3*df*) level. Continuous line: Fit performed with equation $B_{cent}(r) = B_e/[1 + a_1 z + a_2 z^2]$ with $z = \beta(r\text{-}r_e)$. See text.

Table S4. *B*e, a_1 and a_2 parameters determined for the different functionals employed.

DFT	*B*e [cm^{-1}]	a_1	a_2
M11-L	0.068	7.4×10^{-2}	9.2×10^{-3}
M06-2X	0.066	7.2×10^{-2}	7.8×10^{-3}
BMK	0.064	5.0×10^{-2}	1.4×10^{-2}
CAM-B3LYP	0.065	4.9×10^{-2}	1.7×10^{-2}
M08-HX	0.066	7.1×10^{-2}	8.0×10^{-3}
MN12-L	0.066	8.4×10^{-2}	4.8×10^{-3}
MN12-SX	0.064	4.2×10^{-2}	1.2×10^{-2}
MN15-L	0.065	7.9×10^{-2}	3.8×10^{-3}
PW6B95	0.065	4.7×10^{-2}	1.7×10^{-2}
ωB97X-D	0.065	5.9×10^{-2}	1.3×10^{-2}
SOGGA11	0.064	6.9×10^{-2}	1.0×10^{-2}
Mean ± σ	**0.065 ± 0.001**	**$(6.3 \pm 1.5) \times 10^{-2}$**	**$(1.1 \pm 0.5) \times 10^{-2}$**

Table S5. High pressure limit rate constants (in cm^3 $molecule^{-1}$ s^{-1}) as a function of the temperature (in K), calculated for the $CCl_2 + NO_2 \rightarrow CCl_2NO_2$ reaction (channel 1) with SSACM formalism. $F_{AM}^{*} = 6.48$, $\sigma^{*} = 4.0$ and $D_e = 46.3$ kcal mol^{-1} (calculated as $\Delta H_r(0\ K)$ – (ZPE(CCl_2) + ZPE(NO_2)) - ZPE(CCl_2NO_2)). Q_{NO2} and Q_{CCl2}: Ro-vibrational partition functions.

T	Q_{NO2}	Q_{CCl2}	Q_v	Q_m	Q_{cent}	f_{rigid}	$k_{1,\infty}$
300	2.06×10^3	2.08×10^4	1.49	7.39×10^4	5.93×10^3	3.7×10^{-3}	8.73×10^{-13}
500	4.90×10^3	6.77×10^4	2.70	3.66×10^5	9.58×10^3	4.5×10^{-3}	1.33×10^{-12}
1000	2.17×10^4	5.34×10^5	12.78	2.52×10^6	1.82×10^4	4.4×10^{-3}	1.74×10^{-12}
1500	6.58×10^4	2.22×10^6	49.61	6.19×10^6	2.65×10^4	3.3×10^{-3}	1.57×10^{-12}
2000	1.62×10^5	6.56×10^6	155.40	9.85×10^6	3.45×10^4	2.3×10^{-3}	1.22×10^{-12}

Table S6. High pressure limit rate constants (in cm^3 $molecule^{-1}$ s^{-1}) as a function of the temperature (in K), calculated for the $CCl_2 + NO_2 \rightarrow CCl_2NO_2$ reaction (channel 1) according the SACM/CT formalism. $D_e = 46.3$ kcal mol^{-1} (calculated as $\Delta H_r(0\ K)$ – (ZPE(CCl_2) + ZPE(NO_2)) - ZPE(CCl_2NO_2)).

T	f_{rigid}	$k_{1,\infty}$
300	2.9×10^{-3}	7.63×10^{-13}
500	3.6×10^{-3}	1.16×10^{-12}
1000	4.9×10^{-3}	2.04×10^{-12}
1500	5.8×10^{-3}	2.82×10^{-12}
2000	6.5×10^{-3}	3.55×10^{-12}

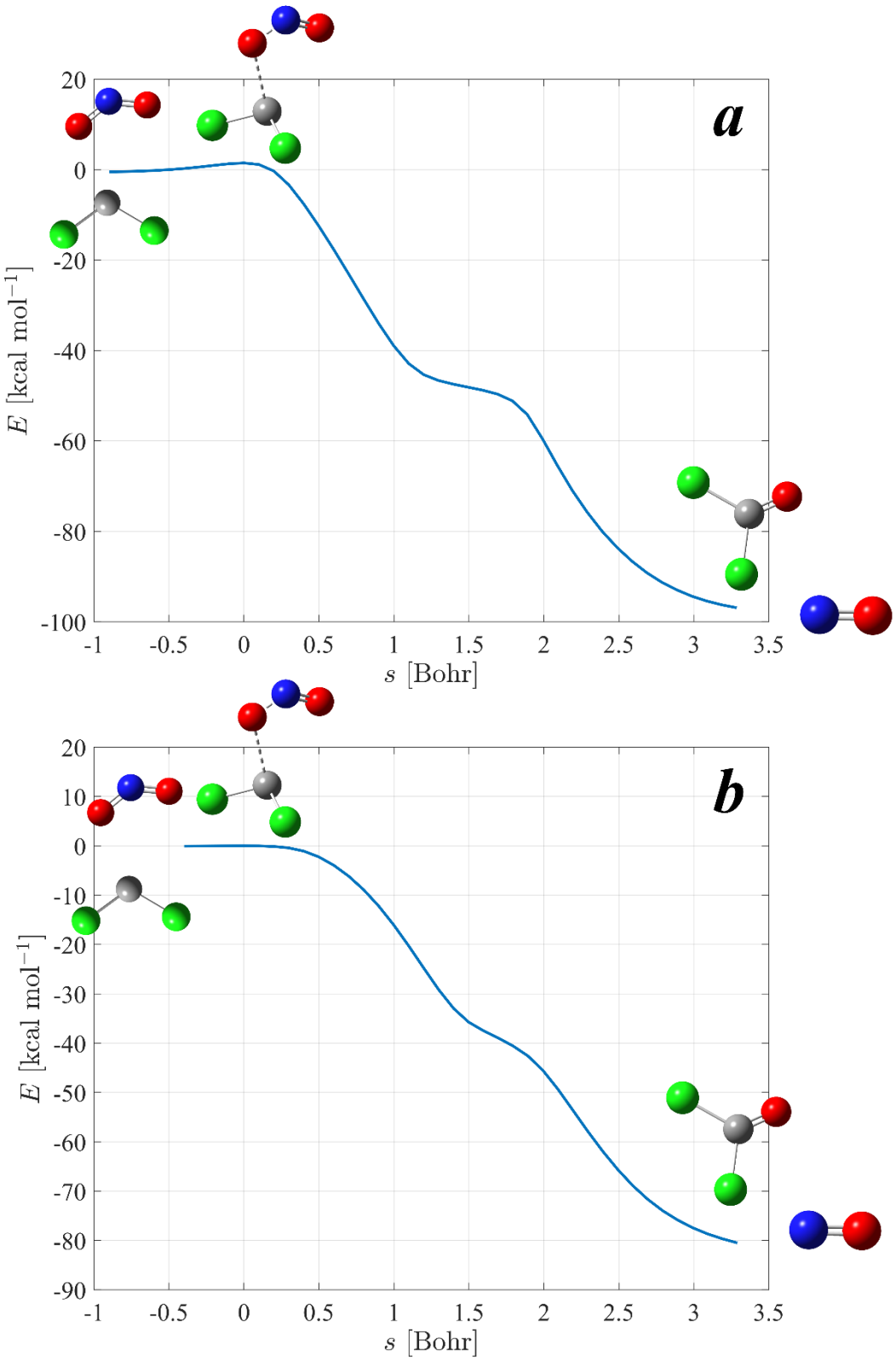

Figure S5. Intrinsic Reaction Coordinate calculation of reaction $CCl_2 + NO_2 \rightarrow CCl_2O + NO$ following transition state TS2a. a) M06-2X/6-311+G(3*df*) level of theory. b) M11-L/6-311+G(3*df*) level of theory.

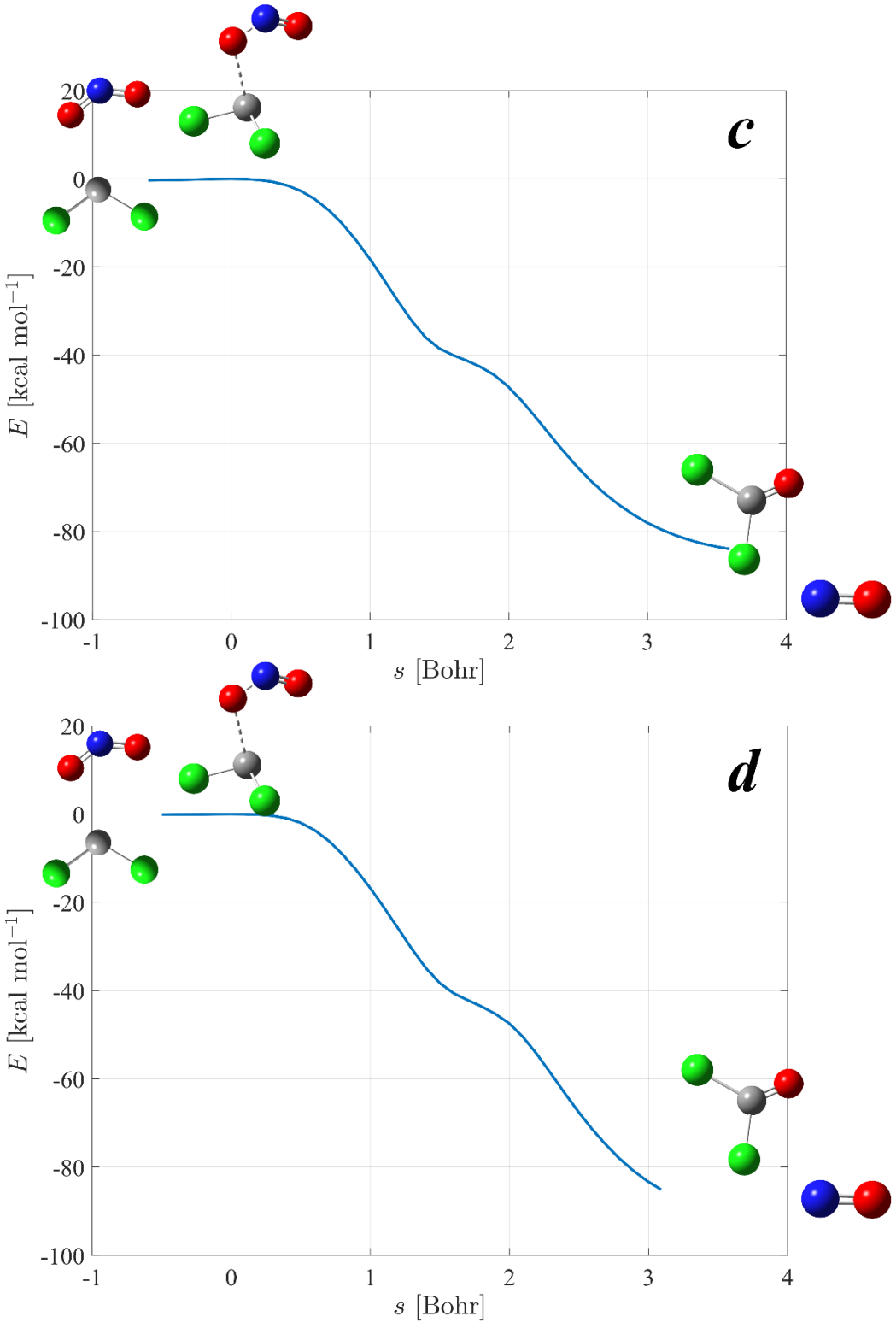

Figure S5 (cont.). Intrinsic Reaction Coordinate calculation of reaction $CCl_2 + NO_2 \rightarrow CCl_2O + NO$ following transition state TS2a. c) MN15-L/6-311+G(3*df*) level of theory. d) PW6B95/6-311+G(3*df*) level of theory.

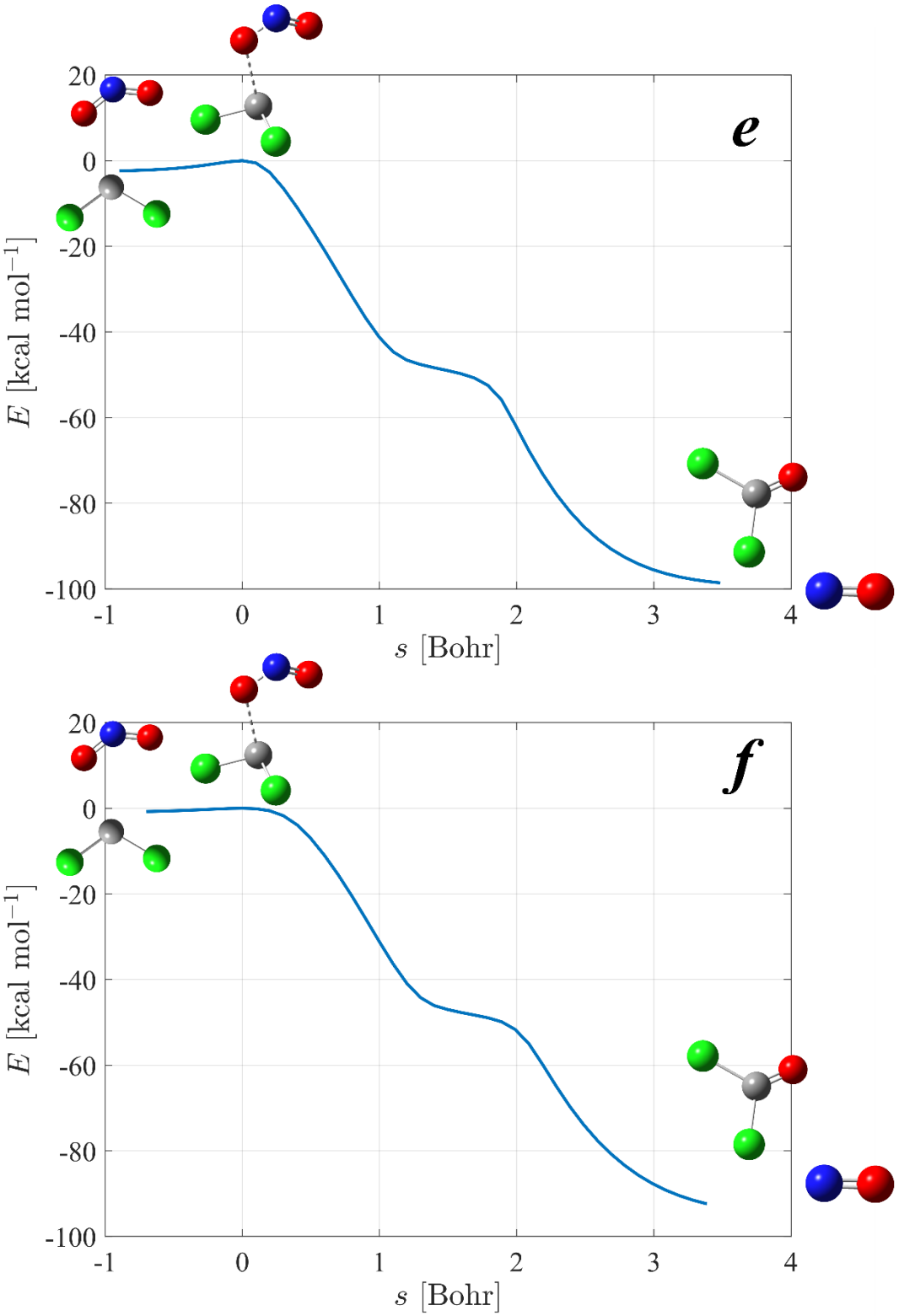

Figure S5 (cont.). Intrinsic Reaction Coordinate calculation of reaction $CCl_2 + NO_2 \rightarrow CCl_2O + NO$ following transition state TS2a. e) M08-HX/6-311+G(3*df*) level of theory. f) MN15/6-311+G(3*df*) level of theory.

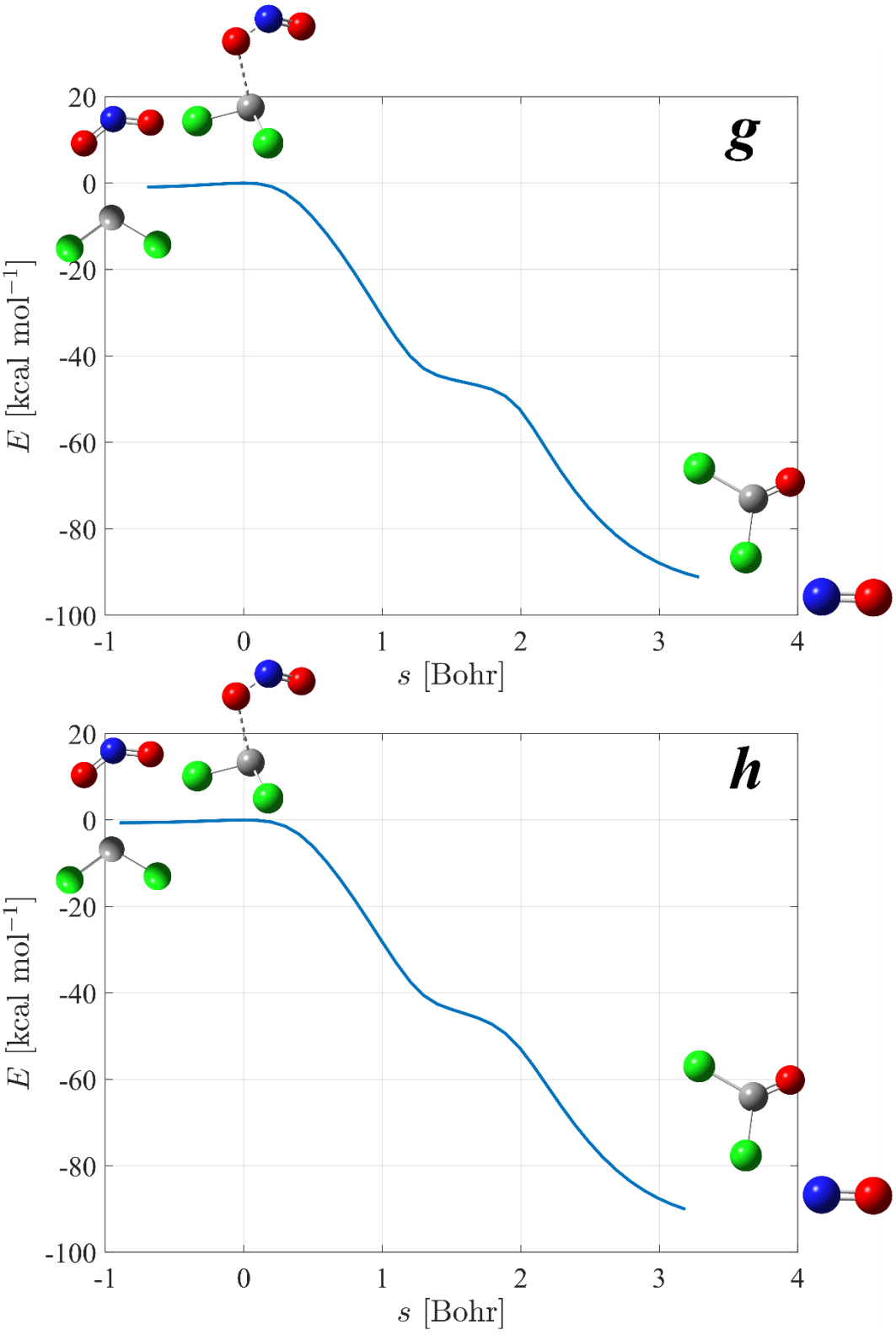

Figure S5 (cont.). Intrinsic Reaction Coordinate calculation of reaction $CCl_2 + NO_2 \rightarrow CCl_2O + NO$ following transition state TS2a. g) MN12-SX/6-311+G(3*df*) level of theory. h) ωB97X-D/6-311+G(3*df*) level of theory.

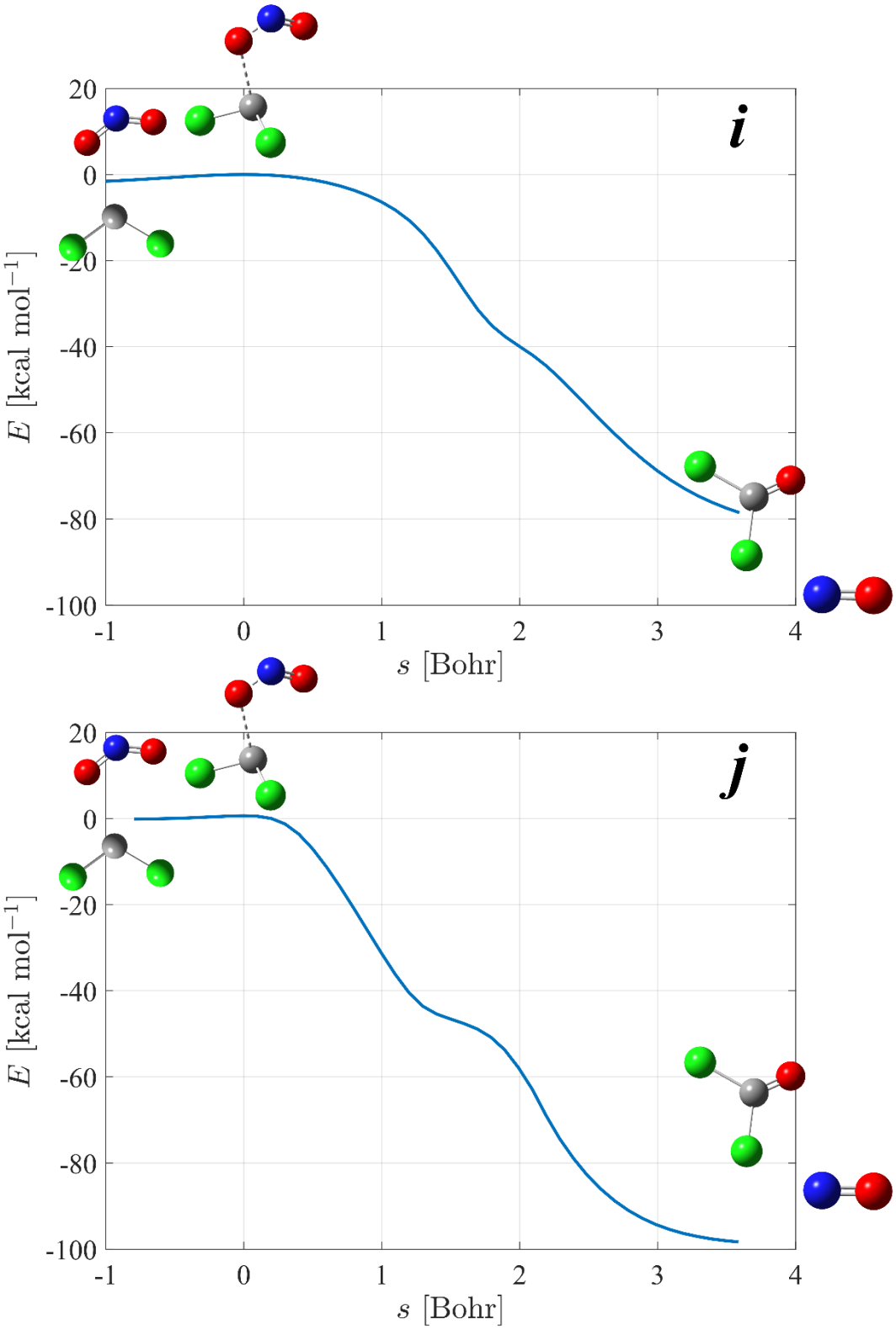

Figure S5 (cont.). Intrinsic Reaction Coordinate calculation of reaction CCl_2 + NO_2 → CCl_2O + NO following transition state TS2a. i) SOGGA11/6-311+G(3*df*) level of theory. j) BMK/6-311+G(3*df*) level of theory.

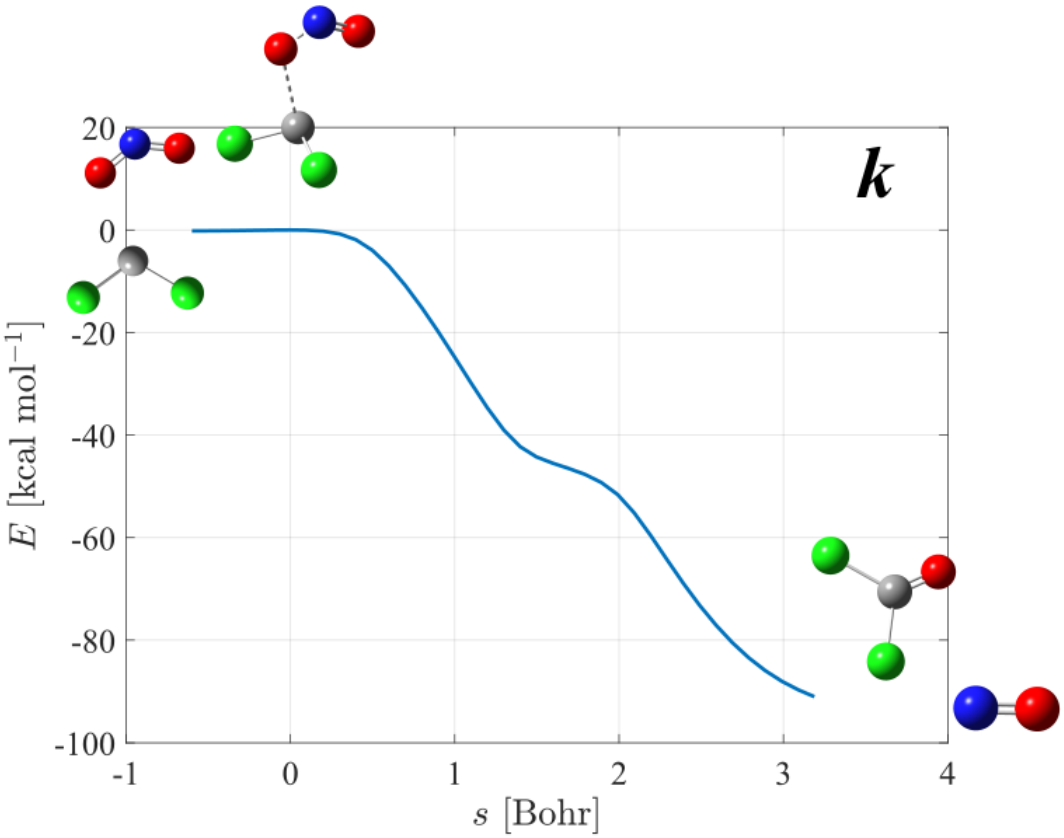

Figure S5 (cont.). Intrinsic Reaction Coordinate calculation of reaction CCl_2 + NO_2 → CCl_2O + NO following transition state TS2a. k) CAM-B3LYP/6-311+G(3*df*) level of theory.

Table S7. Barrier height (TS2a) of the $CCl_2 + NO_2 \rightarrow CCl_2O + NO$ reaction (channel 2) (in kcal mol^{-1}). b: 6-311+G(3*df*).

Chemistry Models	$\Delta H_0^{\ddagger}$	**Chemistry Models**	$\Delta H_0^{\ddagger}$
M06-2X/b	-0.21	G4(MP2)//MN12-L /b	-0.06
MN15/b	-1.12	G4(MP2)//MN12-SX /b	3.03
M11-L/b	-1.79	G4(MP2)//MN15-L /b	1.83
M08-HX/b	-0.08	G4(MP2)//ωB97X-D /b	3.18
PW6B95/b	-0.61	G4(MP2)//SOGGA11/b	1.07
BMK/b	0.91	G4(MP2)//CAM-B3LYP/b	2.67
MN12-L/b	-2.74	G4//M06-2X/b	2.87
MN12-SX/b	-1.34	G4//MN15/b	2.73
MN15-L/b	-2.78	G4//M11-L/b	1.12
ωB97X-D/b	-0.25	G4//M08-HX/b	2.78
SOGGA11/b	1.15	G4//PW6B95/b	0.91
CAM-B3LYP/b	-0.34	G4//BMK/b	3.14
G4(MP2)//M06-2X/b	3.10	G4//MN12-L/b	0.07
G4(MP2)//MN15/b	2.83	G4// MN12-SX/b	2.88
G4(MP2)//M11-L /b	1.27	G4// MN15-L/b	1.63
G4(MP2)//M08-HX/b	3.02	G4//ωB97X-D/b	2.97
G4(MP2)//PW6B95/b	0.96	G4//SOGGA11/b	0.96
G4(MP2)//BMK/b	3.35	G4//CAM-B3LYP/b	2.43

Table S8. Rate constants (in cm^3 $molecule^{-1}$ s^{-1}) calculated for the $CCl_2 + NO_2 \rightarrow CCl_2O + NO$ reaction (channel 2a) at 300 K using the energetics derived from the G4//DFT/6-311+G(3*df*) level of theory. The employed barrier heights are listed in Table S7 of the Supplementary Information.

Level of theory	$k_{2,\infty}$	Level of theory	$k_{2,\infty}$
G4//M06-2X	2.38×10^{-16}	G4//MN15	3.24×10^{-16}
G4//M11-L	1.47×10^{-14}	G4//M08-HX	2.36×10^{-16}
G4//PW6B95	2.70×10^{-14}	G4//BMK	4.67×10^{-16}
G4//MN12-SX	3.41×10^{-16}	G4//CAM-B3LYP	1.79×10^{-15}
G4//MN12-L	3.32×10^{-16}	G4//ωB97X-D	6.41×10^{-16}
G4//MN15-L	1.92×10^{-15}	G4//SOGGA11	4.40×10^{-14}

Table S9. Rate constants (in cm^3 $molecule^{-1}$ s^{-1}) calculated for the $CCl_2 + NO_2 \rightarrow CCl_2O + NO$ reaction (channel 2) at 300-2000 K employing the G4//DFT/6-311+G(3*df*) level of theory (DFT = M06-2X, M08-HX, PW6B95, BMK, MN12-L, MN12-SX, MN15-L, ωB97X-D, SOGGA11, M11-L, CAM-B3LYP).

T [K]	$k_{2,\infty}$				
	M06-2X	M08-HX	PW6B95	BMK	MN12-L
300	2.38×10^{-16}	2.36×10^{-16}	2.70×10^{-14}	4.67×10^{-16}	3.32×10^{-16}
400	1.28×10^{-15}	1.20×10^{-15}	6.89×10^{-14}	2.91×10^{-15}	5.85×10^{-16}
500	4.07×10^{-15}	3.69×10^{-15}	1.41×10^{-13}	1.01×10^{-14}	9.57×10^{-16}
600	9.73×10^{-15}	8.64×10^{-15}	2.50×10^{-13}	2.56×10^{-14}	1.47×10^{-15}
700	1.95×10^{-14}	1.70×10^{-14}	4.06×10^{-13}	5.35×10^{-14}	2.14×10^{-15}
800	3.47×10^{-14}	3.00 c 10^{-14}	6.17×10^{-13}	9.82×10^{-14}	3.01×10^{-15}
900	5.67×10^{-14}	4.85×10^{-14}	8.90×10^{-13}	1.64×10^{-13}	4.08×10^{-15}
1000	8.69×10^{-14}	7.38×10^{-14}	1.24×10^{-12}	2.57×10^{-13}	5.39×10^{-15}
1100	1.27×10^{-13}	1.07×10^{-13}	1.66×10^{-12}	3.80×10^{-13}	6.96×10^{-15}
1200	1.77×10^{-13}	1.49×10^{-13}	2.17×10^{-12}	5.39×10^{-13}	8.81×10^{-15}
1300	2.41×10^{-13}	2.01×10^{-13}	2.78×10^{-12}	7.39×10^{-13}	1.10×10^{-14}
1400	3.18×10^{-13}	2.65×10^{-13}	3.49×10^{-12}	9.84×10^{-13}	1.34×10^{-14}
1500	4.10×10^{-13}	3.41×10^{-13}	4.32×10^{-12}	1.28×10^{-12}	1.63×10^{-14}
1600	5.19×10^{-13}	4.30×10^{-13}	5.26×10^{-12}	1.63×10^{-12}	1.95×10^{-14}
1700	6.47×10^{-13}	5.34×10^{-13}	6.34×10^{-12}	2.04×10^{-12}	2.31×10^{-14}
1800	7.94×10^{-13}	6.54×10^{-13}	7.55×10^{-12}	2.52×10^{-12}	2.71×10^{-14}
1900	9.62×10^{-13}	7.92×10^{-13}	8.91×10^{-12}	3.07×10^{-12}	3.16×10^{-14}
2000	1.15×10^{-12}	9.47×10^{-13}	1.04×10^{-11}	3.70×10^{-12}	3.66×10^{-14}

Table S9 (cont). Rate constants (in cm^3 $molecule^{-1}$ s^{-1}) calculated for the $CCl_2 + NO_2 \rightarrow CCl_2O + NO$ reaction (channel 2) at 300-2000 K employing the G4//DFT/6-311+G(3*df*) level of theory (DFT = M06-2X, M08-HX, PW6B95, BMK, MN12-L, MN12-SX, MN15-L, ωB97X-D, SOGGA11, M11-L, CAM-B3LYP).

T [K]	$k_{2,\infty}$					
	MN12-SX	MN15-L	ωB97X-D	SOGGA11	M11-L	CAM-B3LYP
300	3.41×10^{-16}	1.92×10^{-15}	6.41×10^{-16}	4.40×10^{-14}	1.47×10^{-14}	1.79×10^{-15}
400	1.90×10^{-15}	6.33×10^{-15}	3.69×10^{-15}	1.19×10^{-13}	4.02×10^{-14}	8.40×10^{-15}
500	6.21×10^{-15}	1.51×10^{-14}	1.22×10^{-14}	2.51×10^{-13}	8.55×10^{-14}	2.46×10^{-14}
600	1.51×10^{-14}	2.97×10^{-14}	3.01×10^{-14}	4.56×10^{-13}	1.57×10^{-13}	5.58×10^{-14}
700	3.07×10^{-14}	5.19×10^{-14}	6.16×10^{-14}	7.52×10^{-13}	2.59×10^{-13}	1.08×10^{-13}
800	5.51×10^{-14}	8.32×10^{-14}	1.11×10^{-13}	1.16×10^{-12}	4.00×10^{-13}	1.86×10^{-13}
900	9.07×10^{-14}	1.25×10^{-13}	1.84×10^{-13}	1.68×10^{-12}	5.84×10^{-13}	2.96×10^{-13}
1000	1.40×10^{-13}	1.80×10^{-13}	2.84×10^{-13}	2.35×10^{-12}	8.18×10^{-13}	4.46×10^{-13}
1100	2.05×10^{-13}	2.49×10^{-13}	4.16×10^{-13}	3.18×10^{-12}	1.11×10^{-12}	6.39×10^{-13}
1200	2.88×10^{-13}	3.34×10^{-13}	5.86×10^{-13}	4.18×10^{-12}	1.46×10^{-12}	8.84×10^{-13}
1300	3.92×10^{-13}	4.36×10^{-13}	7.99×10^{-13}	5.38×10^{-12}	1.88×10^{-12}	1.18×10^{-12}
1400	5.19×10^{-13}	5.57×10^{-13}	1.06×10^{-12}	6.78×10^{-12}	2.38×10^{-12}	1.55×10^{-12}
1500	6.72×10^{-13}	7.00×10^{-13}	1.37×10^{-12}	8.41×10^{-12}	2.95×10^{-12}	1.98×10^{-12}
1600	8.52×10^{-13}	8.64×10^{-13}	1.74×10^{-12}	1.03×10^{-11}	3.62×10^{-12}	2.49×10^{-12}
1700	1.06×10^{-12}	1.05×10^{-12}	2.17×10^{-12}	1.24×10^{-11}	4.37×10^{-12}	3.08×10^{-12}
1800	1.31×10^{-12}	1.27×10^{-12}	2.67×10^{-12}	1.48×10^{-11}	5.22×10^{-12}	3.76×10^{-12}
1900	1.59×10^{-12}	1.51×10^{-12}	3.25×10^{-12}	1.75×10^{-11}	6.18×10^{-12}	4.53×10^{-12}
2000	1.90×10^{-12}	1.78×10^{-12}	3.90×10^{-12}	2.05×10^{-11}	7.25×10^{-12}	5.41×10^{-12}

Table S10. Lennard-Jones parameters for various gases [3].

M	**σ [Å]**	**ε/k_B [K]**
He	2.52	9.87
Ne	2.60	75.75
Ar	3.32	143.78
Kr	3.52	207.44
Xe	3.90	262.68
H_2	2.78	64.00
N_2	3.70	84.94
O_2	3.39	121.74

Table S11. Parameters required for the calculation of the rate constant $k_{1,0}$. Z_{LJ} in cm^3 $molecule^{-1}$ s^{-1}. $k_{1,0}$ in cm^6 $molecule^{-2}$ s^{-1}, K_c in molecule cm^{-3}. T in K. $\varepsilon_{CCl2NO2}/k_B$ = 320 K, $\sigma_{CCl2NO2}$ = 5.35 Å, ε_{He}/k_B = 9.87 K and σ_{He} = 2.52 Å [3], ε_{Ar}/k_B = 143.78 K and σ_{Ar} = 3.32 Å [3], ε_{Kr}/k_B = 207.44 K and σ_{Kr} = 3.52 Å [3], ε_{N2}/k_B = 84.94 K and σ_{N2} = 3.70 Å [3]. E_0 = 42.6 kcal mol^{-1}, $\rho_{vib,h}(E_0) = 1.30 \times 10^8$ (kcal $mol^{-1})^{-1}$ and F_{anh} = 1.30.

T	$Z_{LJ} \times 10^{10}$	Q_{vib}	F_E	F_{rot}	F_{rotint}	K_c	β_c	$k_{1,0}$
300	5.93	4.02	1.14	3.14	6.94	8.00×10^{-4}	0.18	[He] 6.72×10^{-29}
	3.75							[Ar] 4.24×10^{-29}
	3.24							[Kr] 3.67×10^{-29}
	4.31							[N_2] 4.88×10^{-29}
500	6.84	19.83	1.25	2.91	4.46	2.3×10^9	0.11	[He] 5.31×10^{-30}
	4.11							[Ar] 3.20×10^{-30}
	3.53							[Kr] 2.74×10^{-30}
	4.79							[N_2] 3.73×10^{-30}
1000	8.44	7.21×10^2	1.63	2.37	2.16	2.45×10^{18}	0.051	[He] 6.83×10^{-32}
	4.84							[Ar] 3.91×10^{-32}
	4.11							[Kr] 3.32×10^{-32}
	5.71							[N_2] 4.62×10^{-32}
1500	9.63	1.25×10^4	2.23	1.98	1.37	1.45×10^{21}	0.027	[He] 3.38×10^{-33}
	5.40							[Ar] 1.89×10^{-33}
	4.56							[Kr] 1.60×10^{-33}
	6.40							[N_2] 2.25×10^{-33}
2000	10.6	1.25×10^5	3.25	1.70	1.00	2.68×10^{22}	0.015	[He] 3.35×10^{-34}
	5.86							[Ar] 1.86×10^{-34}
	4.94							[Kr] 1.56×10^{-34}
	6.97							[N_2] 2.21×10^{-34}

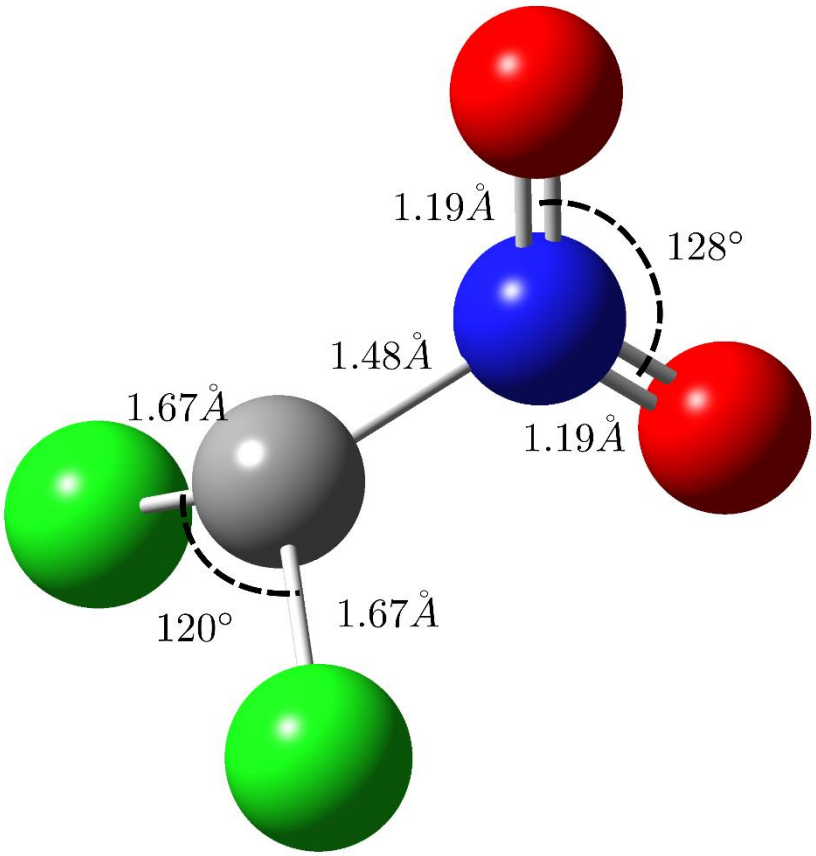

Figure S6. Molecular geometry of the CCl_2NO_2 isomerization transition state calculated at the M11-L/6-311+G(3*df*) level of theory.

Table S12. Modified Kassel parameters and strong collision central broadening factor as a function of the temperature (in K) for the reaction $CCl_2 + NO_2 \rightarrow CCl_2NO_2$.

T	s_k	b_k	F_{cent}^{SC}
300	4.1	12.2	0.45
500	5.7	13.9	0.30
1000	7.9	12.9	0.23
1500	9.0	10.9	0.27
2000	9.7	9.3	0.34

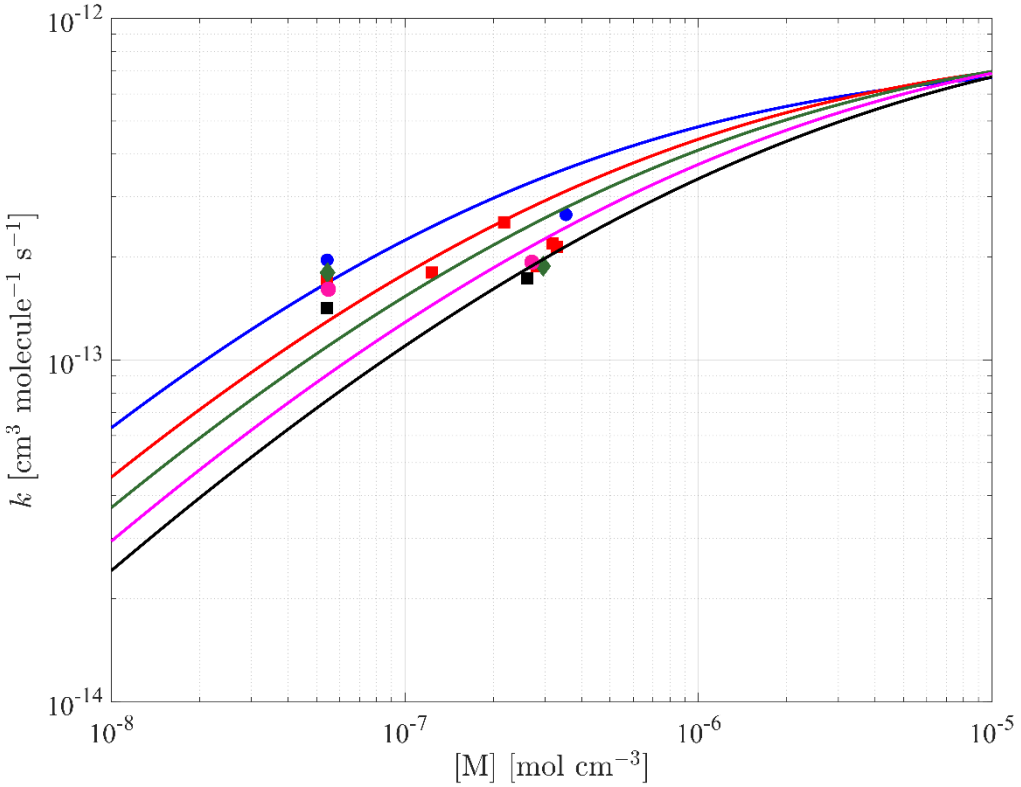

Figure S7. Falloff curves for $CCl_2 + NO_2 + M \rightarrow CCl_2NO_2 + M$ reaction. Solid lines: Results of the calculations of the present work, from up to down T = 266, 298, 318, 340 and 360 K. Experimental results of Eskola et al. [2]: ● 266, ■ 298, ♦ 318, ● 340, and ■ 360 K.

Convergence criteria for geometry optimizations and transition state search

The default configuration of Gaussian16 was used in the implementation of the Self Consistent Field (SCF) method. Direct Inversion in the Iterative Subspace extrapolation method [4] was employed in the determination of the molecular orbitals, and convergence criteria were set to a density matrix root mean square change less than 10^{-8}, and maximum change in the density matrix less than 10^{-6}. Minimizations (optimizations to a local minimum) and optimizations to transition states were performed with the Berny algorithm in redundant internal coordinates. Convergence was tested against criteria for the maximum force component, root-mean square force, maximum step component, and root-mean-square step. The specific convergence criteria used by Gaussian 16 are:

1- The maximum component of the force must be below the cutoff value of 0.00045 hartree/bohr.
2- The root-mean-square of the forces must be below the defined tolerance of 0.0003 hartree/bohr.
3- The calculated maximum displacement for the next step must be smaller than the defined threshold value of 0.0018 bohr.
4- The root-mean-square of the displacement for the next step must be below its cutoff value of 0.0012 bohr.

References

[1] L. A. Curtiss, P. C. Redfern and K. Raghavachari, J. Chem. Phys., 2007, **126**, 084108-1.

[2] A. J. Eskola, I. Golonka, M. P. Rissanen and R. S. Timonen, Chem. Phys. Lett., 2008, **460**, 401.

[3] A. B. Weaver and A. A. Alexeenko, J. Phys. Chem. Ref. Data 2015, **44**, 023103.

[4] P. Pulay, J. Comp. Chem., 1982, **3**, 556-60.